Composites Part B 116 (2017) 40–45

Contents lists available at ScienceDirect

Composites Part B

journal homepage: www.elsevier.com/locate/compositesb

Investigating process-structure relations of ZnO nanofiber via electrospinning method

Ehsan Ghafari [a], Yining Feng [a], Yao Liu [a, b], Ian Ferguson [c], Na Lu [a, *]

[a] Lyles School of Civil Engineering, Sustainable Materials and Renewable Technology (SMART) Lab, Purdue University, USA
[b] Laboratory of Optoelectronic Materials & Detection Technology, Guangxi Key Laboratory for the Relativistic Astrophysics, College of Physics Science & Technology, Guangxi University, China
[c] College of Engineering and Computing, Missouri University of Science and Technology, USA

ARTICLE INFO

Article history:
Received 25 October 2016
Received in revised form
28 November 2016
Accepted 14 February 2017
Available online 20 February 2017

Keywords:
Zinc oxide
Nanofiber
Electrospinning
Size control

ABSTRACT

1D ZnO nanofibers were fabricated in this study using the electrospinning method through sol-gel approach. The effects of fabrication processing parameters on the nanofibers size have been systematically investigated. The higher concentration of the polymer resulted in a broader distribution of the nanofibers diameter due to non-uniform ejection of the fluid jet. The results indicated that an increase in annealing temperature resulted in a lower diameter size and more uniformity of the nanofiber due to decomposition of PVA. The DSC result confirms that an annealing temperature higher than 480 °C is required to remove the PVA and fully decompose the zinc acetate to form crystalline ZnO nano structure. The presence of a crystal ZnO phase was further confirmed by TGA, XRD, FTIR and PL analysis.

1. Introduction

In recent years, there has been a growing interest in developing one dimensional (1D) nanostructures such as nanowires, nanobelts, nanofibers and nanorods due to the ultra-high surface to volume ratio and quantum confinement effect [1–3]. 1D ZnO is one of the most promising oxide nanostructures due to its unique properties and remarkable performance in piezoelectricity [4], photocatalysis [5], and thermoelectricity [6]. In addition, ZnO is low cost, non-toxic and has a large exciton binding energy of 60 meV which makes this material very desirable for a wide range of applications such as light-emitting diodes [7], gas sensors [8–10], solar cell [11,12] and optoelectronics devices [13,14]. 1D ZnO nanofiber have been fabricated by using a variety of methods such as sol-gel [15], electrodeposition [16], hydrothermal [17], vapor phase transport deposition [18], chemical vapor deposition (CVD) [19], and electrospinning [20–25], etc. Among the available methods for synthesizing nanostructures, electrospinning is a simple, versatile and low-cost technique for fabricating flexible nanofibers with significant lengths, uniform diameters in nanoscale and various compositions [26]. Although this method appears to be technically straight-forward, several processing variables need to be well understood and optimized in order to fabricate nanofibers with the desired properties. There have been several studies on the fabrication of ZnO/polymer nanofibers by electrospinning [27–29], however, the effect of processing parameters on the nanofibers size has been rarely investigated. In fact, the ultimate physical and chemical properties of nanofibers are highly dependent on the shape, size and the morphology of the nanofibers. To address this knowledge gap, the current study aims to investigate the effects of polymer concentration, annealing temperature, and annealing time on the size and morphology of the ZnO nanofibers. The morphologies and microstructures of ZnO nanofibers as a function of annealing temperature and solution concentration were analyzed by Thermogravimetric analysis (TGA), x-ray diffraction (XRD), Fourier transform infrared spectroscopy (FTIR) and Photoluminescence (PL) analysis.

2. Experimental procedure

A mixture of ZnO sol–gel solution and poly (vinyl alcohol) (PVA) was used as the precursor for ZnO nanofibers via electrospinning process. Based on a sol–gel approach, 5 g of zinc acetate anhydrous solution of 1 mol was mixed with 15 g of PVA (Mw = 86000) and then stirred for 3 h at 70 °C. The homogenous solution was then

* Corresponding author.
E-mail address: luna@purdue.edu (N. Lu).

http://dx.doi.org/10.1016/j.compositesb.2017.02.026
1359-8368/

added to the 10 ml plastic syringe which was placed in a syringe pump. The positive voltage of 15 kV was applied to the needle to form Tylor cone. The feeding rate of the solution was 0.2 mL/h to obtain a stable liquid jet. The nano fibers were spawned on the aluminum foil substrate, which was placed at a distance of 12 cm from the tip of the needle. The ZnO nanofibers were then annealed

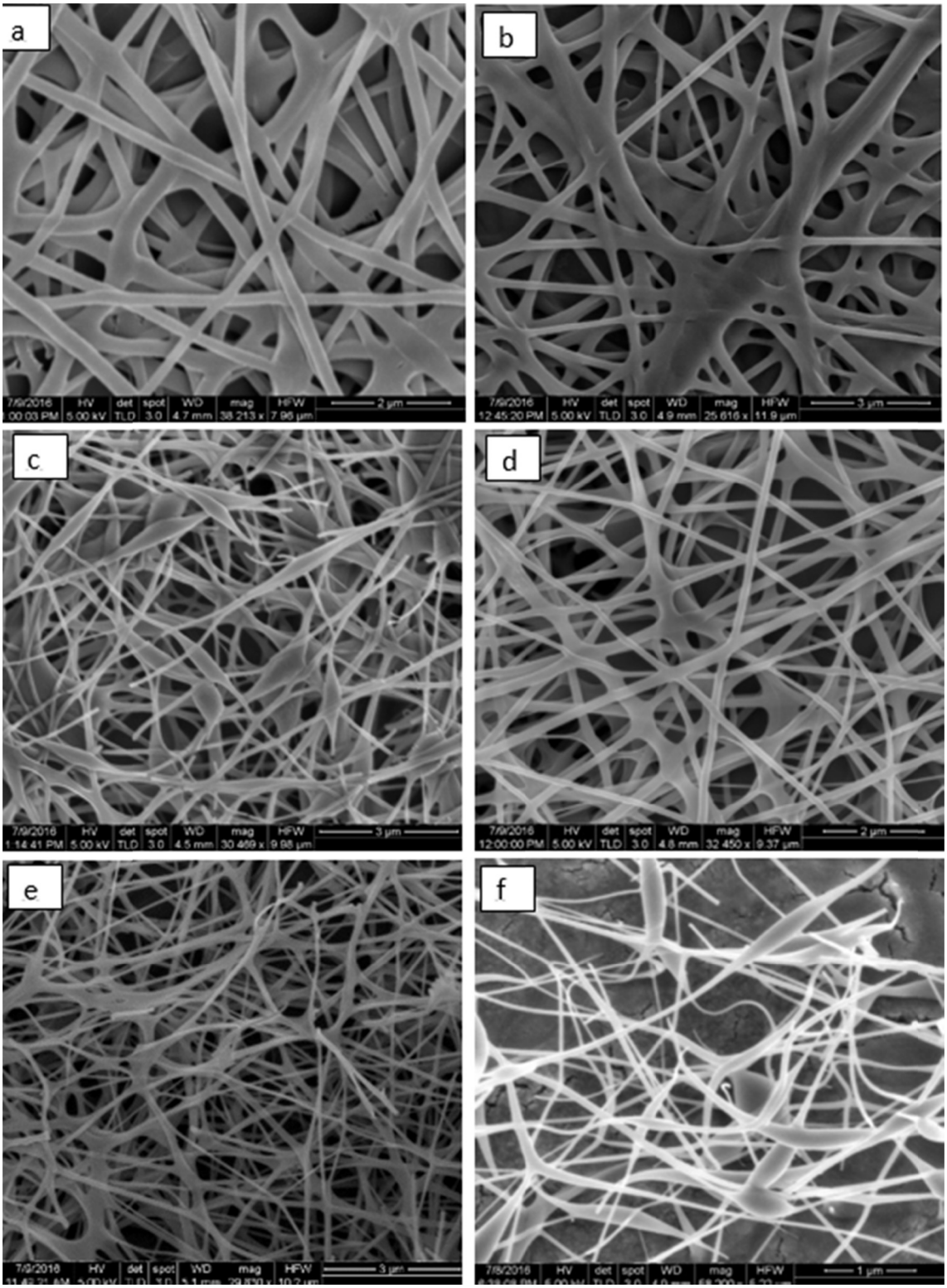

Fig. 1. Scanning electron microscopy image of ZnO fibers: a) as-spun PVA/Zinc acetate nanofibers without thermal annealing with PVA/Zinc acetate ratio = 2 b) as-spun PVA/Zinc acetate nanofibers without thermal annealing with PVA/Zinc acetate ratio = 3; c) beads formation in nanofiber with PVA/Zinc acetate ratio = 4 annealed at 500 °C for 2 h with d) nanofiber with PVA/Zinc acetate ratio = 2 annealed at 300 °C for 2 h; c) nanofiber with PVA/Zinc acetate ratio = 2 annealed at 500 °C; f) nanofiber with PVA/Zinc acetate ratio = 2 annealed at 700 °C.

at four temperatures of 80 °C, 300 °C, 500 °C and 700 °C. The diameter and morphology of the precursor and nanofiber were analyzed using scanning electron microscopy (SEM) and transmission electron microscopy (TEM). TGA and differential scanning calorimetry (DSC) analysis was performed to determine the thermal stability of the precursor fibers. The structure of the ZnO/PVA nanofiber was characterized by XRD, FTIR and PL techniques to analysis the presence of ZnO in the structure of the nanofiber.

3. Results and discussion

3.1. Size controlled of nanofiber

There are several affecting parameters on the diameter of ZnO nanofibers, which can be categorized in three groups as solution properties, electrospinning condition and annealing process. In this study, all the electrospinning parameters such as applied voltage, electrodes distance were kept constant throughout the experiment. However, the effect of polymer concentration, annealing temperature, and annealing time has been studied. SEM was used for visual analysis of the nanofiber microstructure. Fig. 1 shows the SEM image of nanofibers with a fixed content of zinc acetate (1 mol) annealed at different temperatures. A nonwoven structure of nanofiber can be observed in a random orientation for all the samples. The diameter and size distribution of the fibers were analyzed using ImageJ software. The average diameter of ZnO nanofiber as a function of annealing temperature is shown in Fig. 2a, while Fig. 2b presents the average diameter of ZnO nanofiber as function of the annealing durations at 500 °C. As can be seen in Fig. 2a, the diameter of the ZnO nanofiber decreased significantly with the increase of annealing temperature. The average diameter of ZnO nanofiber was around 400 nm without any annealing. However, the average diameter of ZnO nanofiber was found to be 232, 145, 120 and 60 nm with the annealing temperature of 80, 300, 500 and 700 °C, respectively. The decomposition of PVA is the major factor for the shrinkage of the fibers during the annealing process. In addition, the standard deviation of fiber diameter tends to decrease with the increase of temperature which implies the uniform distribution of the fiber in the composite. In order to investigate the annealing time on the on the nanofiber diameter, the samples were annealed at 500 °C for different annealing time (2 h, 4 h, 6 h and 8 h). Fig. 2b shows the effect of annealing time on the nanofiber diameter at 500 °C. As can be seen, the fiber diameter slightly dropped down to 90 nm after 4 h of annealing at 500 °C. However, the results didn't exhibit any significant change in fiber diameter even by increasing the annealing time. In order to study the effect of solution properties, a series of samples with different polymer concentration were made. The viscosity of the electrospinning solution was measured using a DV-I viscometer with No. 3 spindle. Fig. 3 shows the change of fibers diameter and the viscosity as a function of PVA/zinc acetate precursor solutions ratio. A direct relationship can be observed between the PVA/zinc acetate precursor ratio and the viscosity. The viscosity was increased dramatically from 165 cP to 324 cP when more PVA was added to the solution. As shown, the higher viscosity of the solution resulted in a larger fiber diameter. This can be attributed to the higher viscoelastic force of the fluid jet which resists the tension force during the electrospinning process [30]. Furthermore, the increased viscosity resulted in a broader distribution of the nanofibers diameter due to non-uniform ejection of the fluid jet.

The effect of the solution properties on the stability (beads formation) of nanofiber was also studied. Varying the polymer concentration highly affect the nonwoven structure of the nanofiber. For the samples with the viscosity below 325 cP, a lot of beads were observed (See Fig. 1c) in the sample which can be attributed to Rayleigh instability of the fluid jet [31]. In fact, the lower PVDF concentration solution leads to an insufficient viscoelastic force to resist the jet instability.

However, no beads were observed for the solution with the viscosity higher than 325 cP which indicate that the viscoelastic force of the fluid jet suppress the Rayleigh instability [32].

Fig. 4 shows the HR-TEM image of ZnO fibers annealed at 500 °C. It can be observed the sample is comprised of single isolated ZnO grains in Fig. 4a. The diameter of the ZnO fiber shrinks down to about 90 nm. In addition, the crystalline phases are obviously observed in Fig. 4b. As shown, the lattice spacing is 0.262 nm, which matched the interlayer spacing of the (002) planes in the ZnO crystal lattice [33].

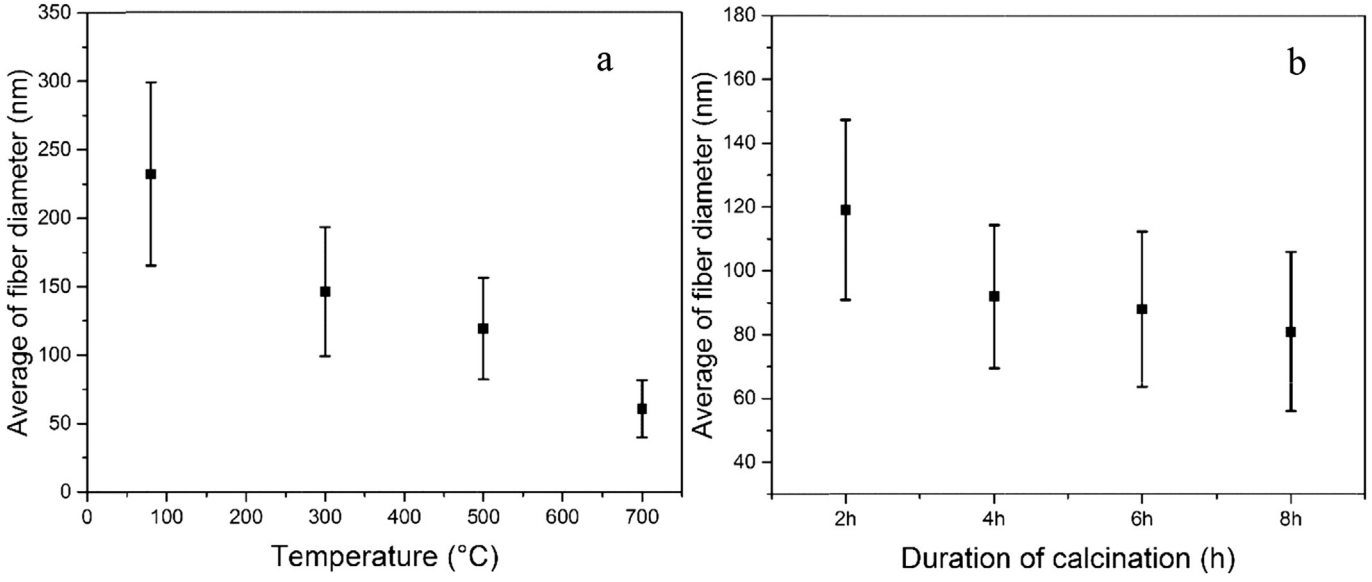

Fig. 2. Diameter of (a) ZnO fibers as a function of annealing temperature (b) ZnO fibers as a function of annealing duration at 500 °C.

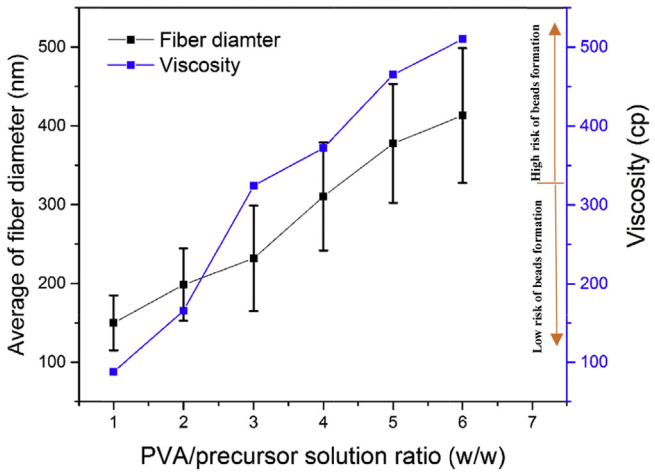

Fig. 3. Diameter of ZnO fibers and viscosity as a function of the PVA/precursor ratio.

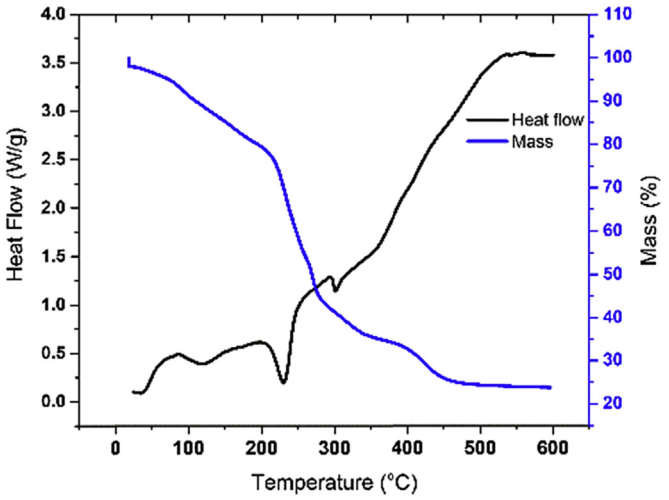

Fig. 5. TGA/DSC analysis of ZnO nanofiber.

3.2. Characterization of nanofiber

The thermal decomposition behavior of ZnO nanofibers was investigated using TGA/DSC analysis from 25 °C to 600 °C at a heating rate of 10 °C/min. The result of TGA/DSC is shown in Fig. 5. The first weight loss (10.80%) is occurred until 110 °C. This weight loss is due to the evaporation of water in the precursor composite fibers. The second weight loss is appeared in a range of 120–480 °C (67.5%). This weight loss is due to the decomposition of PVA and the CH3COOH group of zinc acetate. However, the results indicate that no weight loss occurs above 480 °C, indicating the decomposition of the PVA [34]. As observed in Fig. 5, the endothermic peaks occurred around 120 °C and 240 °C in DSC curve which are attributed to the evaporation of water and decomposition of zinc acetate respective. It has been reported that the crystallization of ZnO occurs around 250 °C through the following reaction [35,36]:

$$Zn\,(CH_3COO)_2 \cdot 2H_2O \;\rightarrow\; Zn\,(CH_3COO)_2 + 2H_2O\uparrow$$
$$Zn\,(CH_3COO)_2 + 2R-OH \;\rightarrow\; ZnO + 2CH_3-CO-R + H_2O$$

The DSC result confirms that the decomposition of the PVA/zinc becomes constant beyond 480 °C, implying that an annealing temperature higher than 480 °C is required to remove the PVA and to fully decompose the zinc acetate into a pure ZnO phase.

In order to determine the interaction between ZnO and PVA, a FTIR analysis was performed. Fig. 6 shows the FT-IR spectra between 4000 and 450 cm $^{-1}$ for the precursor fibers and the Zinc acetate. The band at 3000–3500 cm^{-1} is attributed to the stretch modes of O–H while the appearance the peak at 2937 cm^{-1} is corresponded to the bend and stretching of C-H bonds. The bands at about 1437, 1093, and 850 cm^{-1} are attributed to the stretch modes of C–C, and C–O groups of PVA, respectively. In addition to the vibration bands of PVA, the appearance of vibration band of the Zn–O at 476 cm $^{-1}$ confirms the presence of ZnO in the hybrid fibers (ZnO/PVA) sample. However, all the aforementioned peaks have been disappeared in the annealed nanofiber sample at 500 °C which implies the decomposition of PVA from composite nanofiber. The FTIR spectra clearly exhibits a strong peak at 476 cm $^{-1}$ which confirms the high quality of ZnO crystal structures.

The phase composition and crystal structure of ZnO fibers were further studied using XRD. Fig. 7 shows the XRD diffractograms of

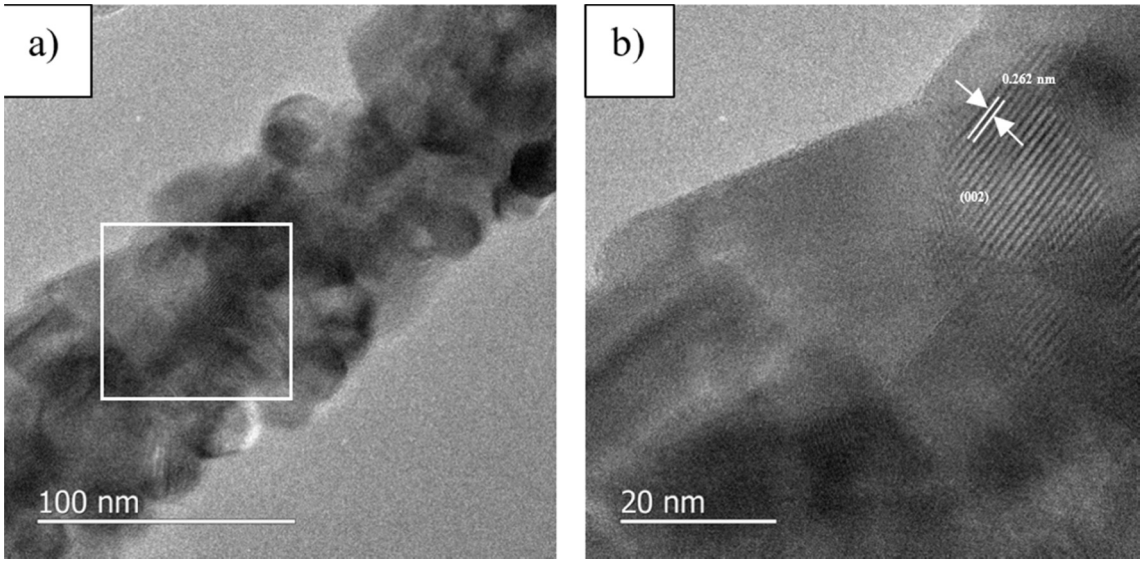

Fig. 4. High Resolution Scanning electron microscopy (HRTEM) image of ZnO fibers annealing at 500 °C.

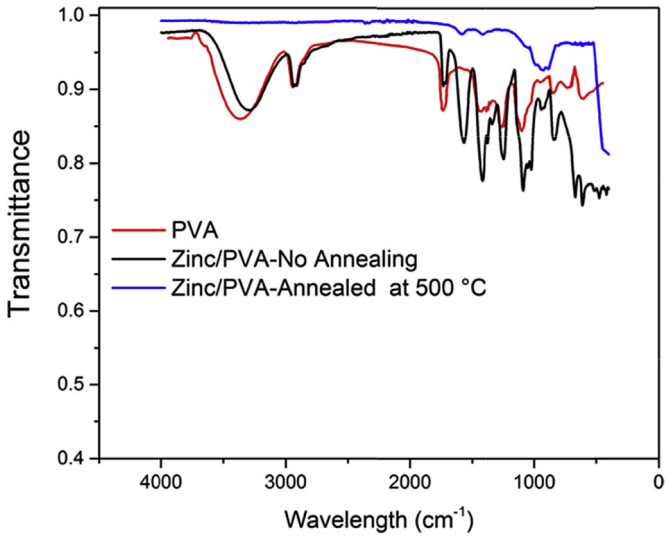

Fig. 6. FTIR analysis of ZnO/PVA nanofiber.

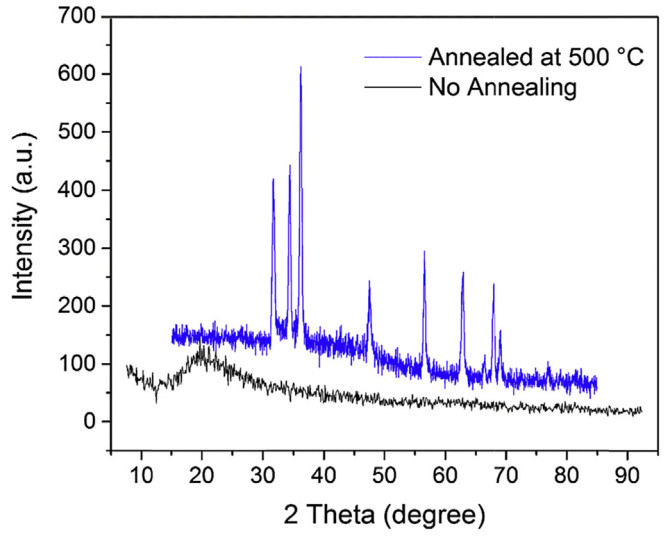

Fig. 7. XRD results for zinc acetate/PVA precursor nanofibers (before annealing) and ZnO nanofibers (after annealing).

the zinc acetate/PVA precursor nanofiber and annealed nanofiber at 500 °C. The XRD diffractograms of zinc acetate/PVA precursor nanofiber shows a broad peak at 2 $\theta = 20°$ which is attributed to semi-crystalline structure of PVA. However, the XRD spectrum of the annealed nanofiber exhibits a well-defined diffraction peaks at 2θ of 31.7°, 34.4°, 36.3°, 47.5° and 56.6° corresponding to (100), (002), (101), (102), (110) plane. All the diffraction peaks clearly indicate the formation of high crystalline zinc oxide with hexagonal wurtzite structure. In addition, the appearance of the ZnO peaks along with the absence of PVA peaks confirm that the high purity of the ZnO nanofiber and decomposition of PVA were realized in the analyzed samples.

PL technology has also been employed to investigate the effect of annealing on the properties of nanofiber. The photoluminescence (PL) measurements were carried out by using a deep ultraviolet (UV) PL spectroscopy. The deep UV PL spectroscopy (Photon Systems Inc.) used here consists of a HeAg laser with an excitation photon energy at around 5.53eV (224 nm), a monochromator (0.25 m), and an integrated photomultiplier (PMT)

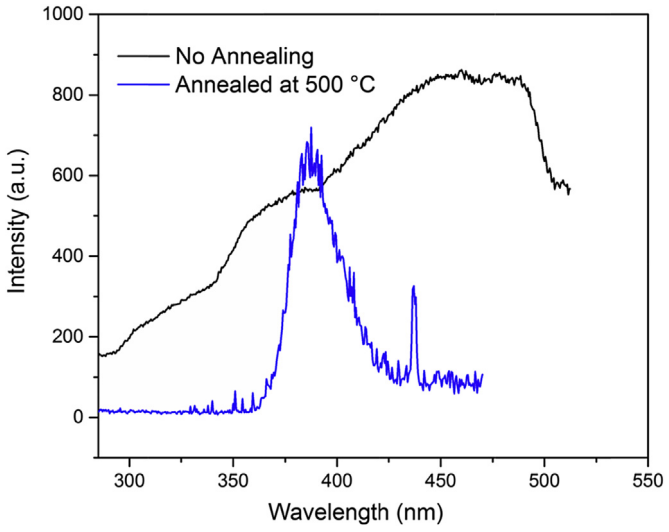

Fig. 8. Photoluminescence spectra of zinc acetate/PVA precursor nanofibers (before annealing) and ZnO nanofibers (after annealing).

detection with the wavelength range of 224–850 nm and a resolution of 0.1 nm. Fig. 8 shows the room temperature PL spectra of the zinc acetate/PVA precursor nanofiber and annealed ZnO nanofiber at 500 °C. For the annealed ZnO nanofiber at 500 °C, one UV emission peak can be seen at about 387 nm (3.2eV) with the FWHM of 239 meV, corresponding to the free exciton emission of ZnO [37], since the transition energy of free exciton emission is lower than the band-gap transition energy of 3.37eV. For the zinc acetate/PVA precursor nanofiber, a broad and intense emission peak can be investigated at the wavelengths approximately from 470 to 520 nm, which may be induced by PVA in zinc acetate/PVA composite [38]. The spectra result not only confirms the presence of ZnO phase but also indicate the decomposition of PVA for the annealed ZnO nanofiber at 500 °C. The PL spectra is also in good agreement with all other experimental results including XRD pattern, FTIR and TGA.

4. Conclusion

In this paper, the high crystal ZnO nanofiber was successfully fabricated using electrospinning method. The effect of solution properties and annealing process on the fiber diameter was investigated. The higher concentration of the polymer not only resulted in a larger diameter of nanofiber but also leads to a broader distribution of the nanofibers diameter due to non-uniform ejection of the fluid jet. The results indicated that an increase in annealing temperature resulted in a lower diameter size and more uniformity of the nanofiber due to decomposition of PVA. The TGA/DSC result confirms that an annealing temperature higher than 480 °C is required to remove the PVA and fully decompose the zinc acetate into a pure ZnO phase. The optimum annealing temperature and duration was found to be 500 °C and 2 h, respectively. No significant change in nanofiber diameter and structure have been observed after 2 h annealing at 500 °C. The presence of the high crystal ZnO nanostructures was confirmed by HRTEM, TGA, XRD, FTIR and PL analysis.

Acknowledgements

The authors at Purdue University are grateful to the funding supports from National Science Foundation (NSF CMMI – 1560834) and Purdue Research Foundation.

References

[1] Yu Y, Xu D. Single-crystalline TiO2 nanorods: highly active and easily recycled photocatalysts. Appl Catal B Environ 2007;73(1–2):166–71.
[2] Dai H. Carbon nanotubes: opportunities and challenges. Surf Sci 2002;500(1):218–41.
[3] Son DI, Yang Hee, Yeon Kim, Tae Whan, Park Il Won. Transparent and flexible ultraviolet photodetectors based on colloidal ZnO quantum dot/graphene nanocomposites formed on poly (ethylene terephthalate) substrates. Compos Part B Eng 2015;69:154–8.
[4] Wang Z, Song J. Piezoelectric nanogenerators based on zinc oxide nanowire arrays. Science 2006;312(5771):242–6.
[5] Matsubara K, Fons P, Iwata K, Yamada A, Sakurai K, Tampo H, et al. ZnO transparent conducting films deposited by pulsed laser deposition for solar cell applications. Thin Solid Films 2003;(431–432):369–72.
[6] Kucukgok B, Wang B, Melton AG, Lu N, Ferguson IT. Comparison of thermoelectric properties of GaN and ZnO samples. Phys status solidi C 2014;11(3–4):894–7.
[7] Tsukazaki A, Ohtomo A, Onuma T, Ohtani M, Makino T, Sumiya M, et al. Repeated temperature modulation epitaxy for p-type doping and light-emitting diode based on ZnO. Nat Mater 2005;4(1):42–6.
[8] Rahman MM, Khan Sher Bahadar, Asiri Abdullah M, Marwani Hadi M, Qusti Abdullah H. Selective detection of toxic Pb (II) ions based on wet-chemically prepared nanosheets integrated CuO–ZnO nanocomposites. Compos Part B Eng 2013;54:215–23.
[9] Abideen ZU, Katoch Akash, Kim Jae-Hun, Kwon Yong Jung, Kim Hyoun Woo, Kim Sang Sub. Excellent gas detection of ZnO nanofibers by loading with reduced graphene oxide nanosheets. Sens. Actuators B Chem 2015;221:1499–507.
[10] Bai S, Chen Song, Zhao Yangbo, Guo Teng, Luo Ruixian, Li Dianqing, et al. Gas sensing properties of Cd-doped ZnO nanofibers synthesized by the electrospinning method. J Mater Chem A 2014;2(39):16697–706.
[11] Zhang Q, Dandeneau C, Zhou X, Cao G. ZnO nanostructures for dye-sensitized solar cells. Adv Mater 2009;21(41):4087–108.
[12] Li X, Li Chaoyang, Hou Shengwen, Hatta Akimitsu, Yu Jinhong, Jiang Nan. Thickness of ITO thin film influences on fabricating ZnO nanorods applying for dye-sensitized solar cell. Compos Part B Eng 2015;74:147–52.
[13] Özgür Ü, Alivov Y, Liu C, Teke A, Reshchikov M, Doğan S, et al. A comprehensive review of ZnO materials and devices. J Appl Phys 2005;98(4):041301.
[14] Liu J, Zhang Zhiyong, Lv Yuanyuan, Yan Junfeng, Yun Jiangni, Zhao Wu, et al. Synthesis and characterization of ZnO NWAs/graphene composites for enhanced optical and field emission performances. Compos Part B Eng 2016;99:366–72.
[15] Kim Y, Tai W, Shu S. Effect of preheating temperature on structural and optical properties of ZnO thin films by sol–gel process. Thin Solid Films 2005;491(1):153–60.
[16] Leprince-Wang Y, Yacoubi-Ouslim A, Wang GY. Structure study of electrodeposited ZnO nanowires. Microelectron J 2005;36(7):625–8.
[17] Sun Y, Ndifor-Angwafor N, Riley D, Ashfold M. Synthesis and photoluminescence of ultra-thin ZnO nanowire/nanotube arrays formed by hydrothermal growth. Chem Phys Lett 2006;431(4):352–7.
[18] Chen B, Sun XW, Xu CX, Tay BK. Growth and characterization of zinc oxide nano/micro-fibers by thermal chemical reactions and vapor transport deposition in air. Phys E Low-dimensional Syst Nanostructures 2004;21(1):103–7.
[19] Xiang B, Wang P, Zhang X, Dayeh S, Aplin D, Soci C, et al. Rational synthesis of p-type zinc oxide nanowire arrays using simple chemical vapor deposition. Nano Lett 2007;7(2):323–8.
[20] Yu H, Fan Huiqing, Wang Xin, Wang Jing. Synthesis and optical properties of Co-doped ZnO nanofibers prepared by electrospinning. Optik-International J Light Electron Opt 2014;125(10):2361–4.
[21] Samanta P, Bagchi Sudeshna, Mishra Sunita. Synthesis and sensing characterization of ZnO nanofibers prepared by electrospinning. Mater Today Proc 2015;2(9):4499–502.
[22] Liu X, Lu Qifang, Liu Jinhua. Electrospinning preparation of one-dimensional ZnO/Bi 2 WO 6 heterostructured sub-microbelts with excellent photocatalytic performance. J Alloy. Compd 2016;662:598–606.
[23] Das AK, Kar Manoranjan, Srinivasan Ananthakrishanan. Room temperature ferromagnetism in undoped ZnO nanofibers prepared by electrospinning. Phys B Condens Matter 2014;448:112–4.
[24] Hong K-S, Kim Jong Wook, Bae Jong-Seong, Hong Tae Eun, Jeong Euh Duck, Jin Jong Sung, et al. Structure, chemical bonding states, and optical properties of the hetero-structured ZnO/CuO prepared by using the hydrothermal and the electrospinning methods. Phys B Condens Matter 2017;504:103–8.
[25] Di Mauro A, Zimbone Massimo, Fragalà Maria Elena, Impellizzeri Giuliana. Synthesis of ZnO nanofibers by the electrospinning process. Mater Sci Semicond Process 2016;42:98–101.
[26] Deitzel JM, Kleinmeyer James, Harris DEA, Tan NC Beck. The effect of processing variables on the morphology of electrospun nanofibers and textiles. Polymer 2001;42(1):261–72.
[27] Park J, Moon J, Lee S, Lim S, Zyung T. Fabrication and characterization of ZnO nanofibers by electrospinning. Curr Appl Phys 2009;9(3):S210–2.
[28] Liu H, Yang J, Liang J, Huang Y, Tang C. ZnO nanofiber and nanoparticle synthesized through electrospinning and their photocatalytic activity under visible light. J Am Ceram Soc 2008;91(4):1287–91.
[29] Zhao M, Wang X, Ning L, He H, Jia J, Zhang L, et al. Synthesis and optical properties of Mg-doped ZnO nanofibers prepared by electrospinning. J Alloy. Compd 2010;507(1):97–100.
[30] Nezarati RM, Eifert MB, Cosgriff-Hernandez E. Effects of humidity and solution viscosity on electrospun fiber morphology. Tissue Eng Part C Methods 2013;19(10):810–9.
[31] Shin Y, Hohman MM, Brenner MP, Rutledge GC. Electrospinning: a whipping fluid jet generates submicron polymer fibers. Appl Phys Lett 2001;78(8):1149–51.
[32] Fong H, Chun I, Reneker DH. Beaded nanofibers formed during electrospinning. Polymer 1999;40(16):4585–92.
[33] Andrews SC, Fardy MA, Moore MC, Aloni S, Zhang M, Radmilovic V, Yang P. Atomic-level control of the thermoelectric properties in polytypoid nanowires. Chem. Sci. 2011;2(4):706–14.
[34] Wu H, Pan Wei. Preparation of zinc oxide nanofibers by electrospinning. J Am Ceram Soc 2006;89(2):699–701.
[35] Majumder S, Jain M, Dobal PS, Katiyar RS. Investigations on solution derived aluminium doped zinc oxide thin films. Mater Sci Eng B 2003;103(1):16–25.
[36] Bazargan AM, Fateminia SMA, Ganji ME, Bahrevar MA. Electrospinning preparation and characterization of cadmium oxide nanofibers. Chem. Eng. J. 2009;155(1):523–7.
[37] Zhang J, Wen B, Wang F, Ding Y, Zhang S, Yang M. In situ synthesis of ZnO nanocrystal/PET hybrid nanofibers via electrospinning. J Polym Sci Part B Polym Phys 2011;49(19):1360–8.
[38] Sui XM, Shao CL, Liu YC. White-light emission of polyvinyl alcohol/ ZnO hybrid nanofibers prepared by electrospinning. Appl Phys Lett 2005;87(11):113115.